IOP Publishing   Phys. Scr. 98 (2023) 044004   https://doi.org/10.1088/1402-4896/acb408

Physica Scripta

CrossMark

OPEN ACCESS

RECEIVED
16 October 2022

REVISED
9 January 2023

ACCEPTED FOR PUBLICATION
17 January 2023

PUBLISHED
10 March 2023

PAPER

Observation of Bohm trajectories and quantum potentials of classical waves

Georgi Gary Rozenman[1,2], Denys I Bondar[3], Wolfgang P Schleich[4,5], Lev Shemer[6] and Ady Arie[2]

[1] Raymond and Beverly Sackler School of Physics & Astronomy, Faculty of Exact Sciences, Tel Aviv University, Tel Aviv 69978, Israel
[2] School of Electrical Engineering, Iby and Aladar Fleischman Faculty of Engineering, Tel Aviv University, Tel Aviv 69978, Israel
[3] Department of Physics and Engineering Physics, Tulane University, 6823 St. Charles Avenue, New Orleans, LA 70118, United States of America
[4] Institut für Quantenphysik and Center for Integrated Quantum Science and Technology (IQ^{ST}), Universität Ulm, D-89081 Ulm, Germany
[5] Hagler Institute for Advanced Study at Texas A&M University, Texas A&M AgriLife Research, Institute for Quantum Science and Engineering (IQSE), and Department of Physics and Astronomy, Texas A&M University, College Station, TX 77843-4242, United States of America
[6] School of Mechanical Engineering, Faculty of Engineering, Tel Aviv University, Tel Aviv 69978, Israel

E-mail: garyrozenman@protonmail.com

Keywords: Bohm, trajectories, pilot wave theory, quantum potential, surface gravity waves

Abstract

In 1952 David Bohm proposed an interpretation of quantum mechanics, in which the evolution of states results from trajectories governed by classical equations of motion but with an additional potential determined by the wave function. There exist only a few experiments that test this concept and they employed weak measurement of non-classical light. In contrast, we reconstruct the Bohm trajectories in a classical hydrodynamic system of surface gravity water waves, by a direct measurement of the wave packet. Our system is governed by a wave equation that is analogous to the Schrödinger equation which enables us to transfer the Bohm formalism to classical waves. In contrast to a quantum system, we can measure simultaneously their amplitude and phase. In our experiments, we employ three characteristic types of surface gravity water wave packets: two and three Gaussian temporal slits and temporal Airy wave packets. The Bohm trajectories and their energy flows follow the valleys and bounce off the hills in the corresponding quantum potential landscapes.

1. Introduction

Almost a hundred years ago, that is in 1924, Louis de Broglie proposed an explanation of quantum phenomena based on nonclassical trajectories guided by a wave field [1]. This revolutionary idea was followed by Erwin Madelung's re-formulation [2] of Schrödinger's equation in terms of hydrodynamic variables which provides the foundations of the interpretation of quantum mechanics put forward by David Bohm known as Bohmian mechanics [3, 4]. This theory makes a proposal for how the microscopic world might work that agrees with all tests of quantum mechanics [5]. In contrast to the Copenhagen interpretation [6] which assumes that the wave function determines only the probability of measuring a particle at a certain position, according to Bohmian mechanics, particles have well-defined positions at all times [7], and follow trajectories, known as Bohm's trajectories [8]. Furthermore, in Bohmian mechanics the wave function is used to construct a quantum potential that, when combined with Newton's equations, draws the Bohm trajectories [3].

Comprehensive discussions of Bohmian mechanics, which has recently received renewed attention can be found at several places in the literature [9–13] and many interesting applications beyond the interpretation of quantum mechanics have been proposed. For example, Bohmian mechanics is utilized for a better understanding of the quantum–classical transition [14] as well as, nanoscale electron devices and electron transport in open systems [15]. Bohmian equations sometimes provide more efficient computational tools than those obtained by orthodox methods [16] and are now routinely used in quantum chemistry [17, 18]. In

Table 1. Bohmian mechanics of classical surface gravity water waves motivated by its quantum counterpart. Here t and x denote time and space, whereas τ and ξ are dimensionless transverse and propagation coordinates. In this transition [27] from a quantum wave to a classical surface gravity wave we make the replacements $\hbar \to 1$, $i \to -i$ and $m \to 1/2$.

Quantity	Quantum mechanics	Surface gravity water waves
Complex-valued function	wave function $\psi(x, t)$	surface envelope $A(\tau, \xi)$
Propagation coordinate	t	ξ
Transverse coordinate	x	τ
Wave equation	$i\hbar\frac{\partial\psi}{\partial t} = -\frac{\hbar^2}{2m}\frac{\partial^2\psi}{\partial x^2}$	$i\frac{\partial A}{\partial\xi} = \frac{\partial^2 A}{\partial\tau^2}$
Guiding equation	$\frac{d}{dt}\overline{x}(t) = \frac{\hbar}{m}Im\left\{\frac{1}{\psi(\overline{x}(t),t)}\frac{\partial}{\partial\overline{x}}\psi\right\}$	$\frac{d}{d\xi}\overline{\tau}(\xi) = 2\,Im\left\{\frac{1}{A(\xi,\overline{\tau}(\xi))}\frac{\partial}{\partial\overline{\tau}}A\right\}$
Quantum potential	$Q = -\frac{\hbar^2}{2m}\frac{1}{\mid\psi\mid}\frac{\partial^2}{\partial x^2}\lvert\psi\rvert$	$Q = -\frac{1}{\mid A\mid}\frac{\partial^2}{\partial\tau^2}\lvert A\rvert$

addition, it was recently argued that this formalism can also be employed to gain insight into concepts in cosmology [19].

However, despite being covered by a wide spectrum of different physical systems, an experimental observation of Bohm trajectories is challenging [20] and we are only aware of a few experiments using weak measurements [21, 22] of either single photons [23] or entangled photons [24]. In the present article we study experimentally Bohmian mechanics for a classical system of surface gravity water waves. This unusual application of a concept from quantum mechanics to a classical wave, and its verification by an experiment, is made possible by three physical properties of surface gravity water waves: (i) they obey a wave equation that is analogous to the Schrödinger equation of a quantum particle. (ii) We can define the ingredients of Bohmian mechanics such as trajectories or the quantum potential as demonstrated by table 1, and (iii) it is possible to measure the amplitude *and* determine the phase of a surface gravity water wave [25, 26].

We further emphasize that the ability to reconstruct trajectories of a wave packet is not limited to quantum mechanical waves, but is useful also for classical waves. In fact, intriguing concepts, such as the trajectories in double-slit or multiple-slit wave interference experiments are present for both quantum waves as well as classical surface gravity water waves. Moreover, the measurement we perform does not disturb the propagation dynamics, nor does it cause a collapse of the wave function.

Our article is organized as follows: in section 2 we lay the foundations for the discussion of our experiments on the observation of Bohmian trajectories and quantum potentials corresponding to classical waves. In particular, we compare and contrast typical elements of Bohmian mechanics as defined in quantum theory to the analogous expressions of surface gravity water waves. We then devote section 3 to our experiments and report the time evolution and the quantum potentials for four configurations: (i) The familiar double-slit arrangement with an initial zero transverse momentum, (ii) the three-slit experiment again with zero momentum, (iii) the double-slit version with non-zero momentum, and (iv) a truncated Airy wave packet. We conclude in section 4 by briefly summarizing our results and presenting an outlook.

In order to keep our article concise while self-consistent we have included an appendix. Here we first briefly review the Hilbert transform which allows us to extract the phase of the wave function, and then we provide explicit expressions for the wave packets used in our experiments.

2. Surface gravity water waves

In a frame moving with the group velocity c_g the evolution of the complex-valued envelope $A = A(\tau, \xi)$ of a surface gravity water wave follows from the wave equation

$$i\frac{\partial A}{\partial \xi} = \frac{\partial^2 A}{\partial \tau^2}, \tag{1}$$

reminiscent of the Schrödinger equation of a free particle as summarised in table 1. The scaled dimensionless variables ξ and τ are related to the propagation coordinate x and the time t by $\xi \equiv \varepsilon^2 k_0 x$ and $\tau \equiv \varepsilon\omega_0(x/c_g - t)$. The carrier wave number k_0 and the angular carrier frequency ω_0 satisfy the deep-water dispersion relation $\omega_0^2 = k_0 g$ with g being the gravitational acceleration, and define the group velocity $c_g \equiv \omega_0/2k_0$. The parameter

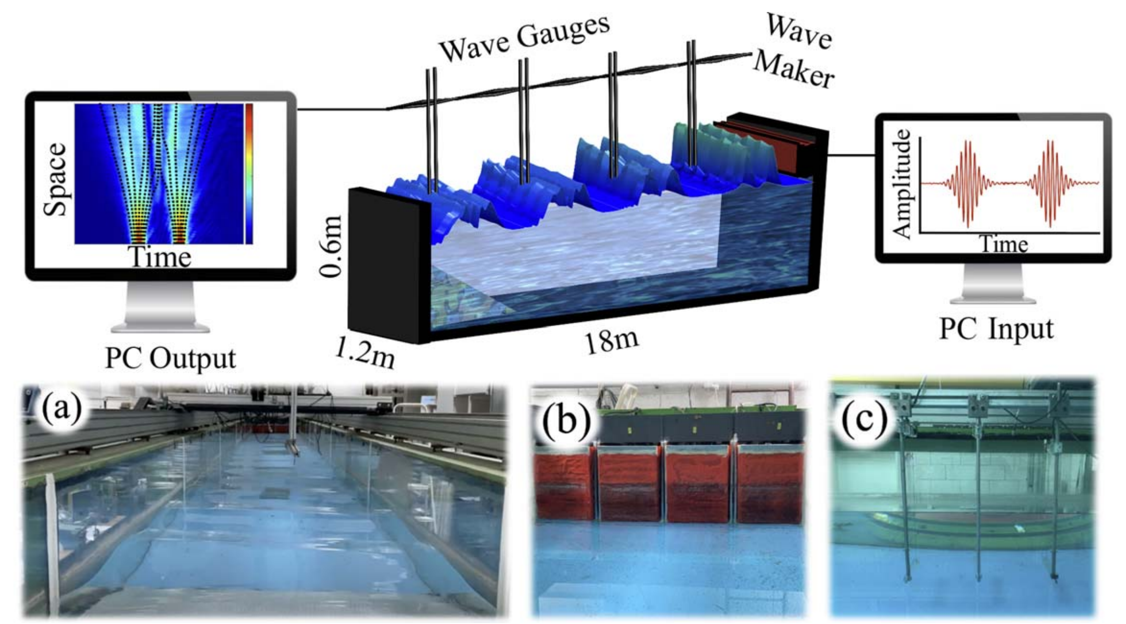

Figure 1. Concept of our experiment to observe Bohm trajectories and the quantum potential of surface gravity water waves (top) and photographs of the key ingredients of the set-up (bottom). At one end of the water tank (a) four computer-controlled wave makers (b) create surface gravity water waves whose elevations are measured by wave gauges (c) based on time-dependent resistance. The wave gauges measure the height of the water surface, practically without disturbing the propagation dynamics. From the collection of envelopes in time and space we reconstruct the Bohm trajectories as well as the quantum potential.

$\varepsilon \equiv k_0 a_0$ characterizing the wave steepness is assumed to be small, that is $\varepsilon \ll 1$, in order to ensure [28] the linearity of the wave equation.

From equation (1) and table 1 we note that for spatially evolving surface gravity water waves, the roles of time and space are interchanged compared to quantum mechanics [29–31]. Hence, the guiding equation

$$\frac{d}{d\xi}\overline{\tau}(\xi) = 2\, Im\left\{\frac{1}{A(\xi,\, \overline{\tau}(\xi))}\frac{\partial}{\partial \tau}A|_{\tau=\overline{\tau}(\xi)}\right\} \tag{2}$$

in terms of the complex-valued amplitude A and its time derivative determines the surface gravity water wave trajectories $\overline{\tau} = \overline{\tau}(\xi)$.

Another way to obtain trajectories in a wave theory is motivated by classical mechanics and involves [7] the quantum potential. For surface gravity water waves this potential reads

$$Q = -\frac{1}{|A|}\frac{\partial^2}{\partial \tau^2}|A|, \tag{3}$$

where $|A|$ is the absolute value of the complex water wave envelope governed by the wave equation equation (1).

We note that the elevation of the surface gravity water wave is real, and connected to the complex envelope A by being its real part. Hence, the imaginary part of A follows from the Hilbert [32] transform of the real-valued elevation, as outlined in the appendix.

3. Experimental realization

The experiments discussed in our article were performed in a 18 m long, 1.2 m wide, and $h = 0.6$ m deep laboratory wave tank shown in figure 1. Water waves are generated by a computer-controlled wave maker placed at one end of the tank. Four wave gauges supported on a bar connected to a computer-controlled carriage measure the elevations of the surface gravity water waves at any location along the tank [25, 26]. For our experiments they are placed at 30 different locations in the region of interest of $0.4 - 12\ m$ to eliminate residual reflections from the absorbing beach placed at the other end of the water tank, resulting in 120 spatial coordinates.

We have used a carrier wave frequency and wave number of $\omega_0 = 9\ rad/s$ and $k_0 = 8.3\ 1/m$ giving rise to a group velocity $c_g = 0.54\ m/s$, and the amplitudes are $a_0 = 6\ mm$ for the two-slit and three-slit experiments, and $a_0 = 5\ mm$ for the self-accelerating Airy wave packet shown in figures 2 and 3. For all cases, k_0 satisfies the deep-water condition [31] $k_0 h > \pi$, and the corresponding steepness is $\varepsilon < 0.05$ guaranteeing the validity of the linear Schrödinger equation.

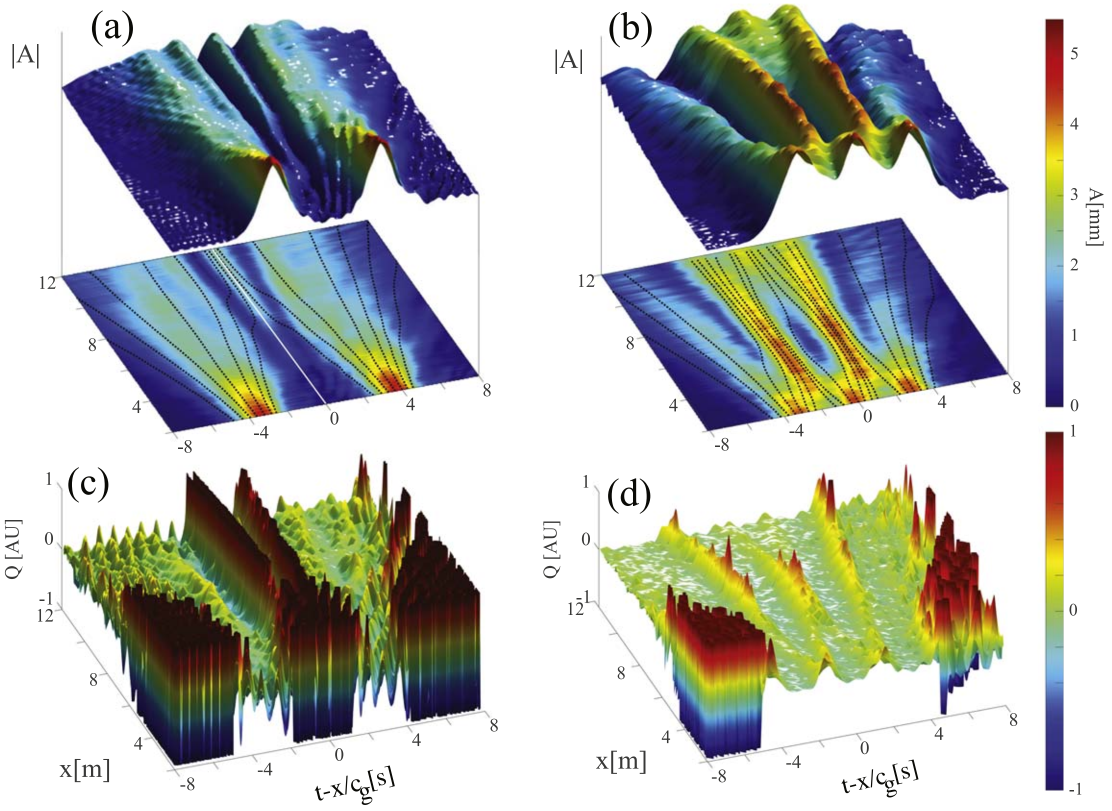

Figure 2. Experimentally obtained surface gravity water wave evolutions (top) and corresponding quantum potentials (bottom) of two-slit (a), (c) and three-slit (b), (d) envelopes $|A|$. Bright and dark colors reflect high and low values, and the color bar units are millimeters. The Bohm trajectories indicated by dashed lines in the 2D-intensity plot underneath (a), (b) and following from equation (2), run in the valleys of the landscape formed by the quantum potentials (c), (d). The tall mountain ranges lead to low amplitudes $|A|$. A key difference between the two-slit and three-slit results is the dark island apparent in the 2D-plot of (b) which the Bohm trajectories seem to avoid, and the corresponding crater in the envelope, both of which result from an additional mountain at the center of the quantum potential (d).

In figures 2 and 3 we show the absolute value $|A|$ of the wave-function analogue in a two- and three-dimensional representation together with the Bohm trajectories using equation (2), as well as the quantum potentials defined by equation (3) for four different wave packets: the two-slit and three-slit experiments with zero momentum in figures 2(a), (b), a two-slit experiment with a non-zero momentum, and a truncated Airy wave packet displayed by figures 3(a), (b).

The temporal-slit experiments were performed with a temporal width of $t_0 = 1.7s$ and temporal distances $t_s = 8\ s$ and $t_s = 4\ s$ for two and three slits, respectively. We note that for the three-slit experiment we chose an initial wave packet with a partial overlap between the wings of the three Gaussian lobes, in order to highlight the appearance of additional features compared to the two-slit experiment. For the explicit form of the wave packets we refer to the appendix.

In figure 2(a) we show the case of two-slit interference, a cornerstone of quantum mechanics. Here the Bohm trajectories are marked by black dashed lines. The average trajectory (white line) follows a straight line in accordance with the Ehrenfest theorem [33, 34], i.e. the average trajectory is identical to the classical propagation of the particle which is in this case stationary owing to the fact that the particle exits a slit with zero momentum.

The interference pattern at the end of the water tank, that is at $x = 12\ m$, is intimately linked to the quantum potential. Figure 2(c) shows that the trajectories avoid the regions of destructive interference where the quantum potential exhibits very high values. In contrast, the trajectories concentrate in the domains of constructive interference, where the quantum potential assumes small values.

For the three-slit experiment displayed in figures 2(b), (d), we observe a spot at $x = 6\ m$ where destructive interference accrues, and the corresponding trajectories avoid this region during propagation. From the view of the quantum potential which is presented in figure 2 (d) this avoidance results from a sharp hill in this region.

Next we examine two slits with an effective initial non-zero momentum [27] $p_0 = -2\ rad/s$. From figure 3 (a) we note that the particles exiting the two slits have Bohm trajectories propagating at a negative constant velocity. The quantum potential shown in figure 3(c), has its repulsive walls shifted in the momentum direction, providing canals of linearly shifted trajectories with the corresponding initial momentum.

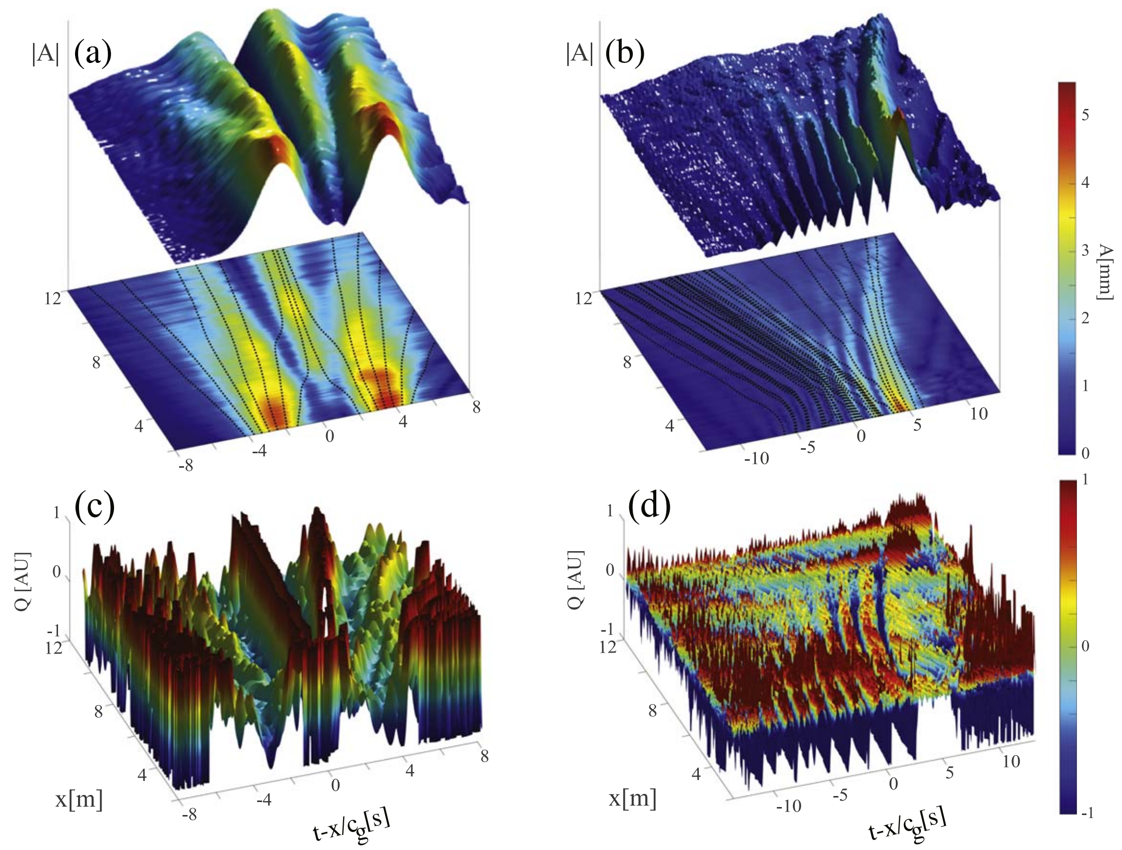

Figure 3. Experimentally obtained surface gravity water wave evolutions (top) and quantum potentials (bottom) of two-slit envelopes with non-zero initial momentum (a), (c) and a truncated Airy wave packet (b), (d). Bright and dark colors reflect high and low values of $|A|$, and the color bar units are millimeters. The Bohm trajectories indicated by dashed lines in the 2D-intensity plot underneath (a) are tilted in comparison to the ones shown in left column of figure 2, and result from the tilted valleys of the quantum potential (c). The quantum potential of the truncated Airy wave packet (d) consists of narrow and rather deep valleys that curve to the right indicating the familiar self-acceleration and guide the Bohm trajectories. However, there also exist trajectories bending to the left and the average trajectory is straight, in complete agreement with the free propagation of the center of mass of the truncated Airy wave packet.

Finally, we study the Airy wave packet which is a solution of the time-dependent Schrödinger equation for a quantum mechanical particle in a linear potential. It was predicted [35] in 1979 and experimentally verified [25, 31, 36–40] for optical, matter and water waves that the wavefronts of freely propagating Airy wave packets self-accelerate and follow a parabolic trajectory. However, in the case of zero initial momentum the center of mass of an Airy wave moves at the group velocity which is zero. For a *pure* Airy wave packet which is infinitely long and non-normalizable there is no contradiction with Ehrenfest's theorem, as the state has an undefined $\langle t \rangle$ for all coordinates.

However, in our experiment we generate *truncated* Airy wave packets with $t_0 = 0.65$ *s* and the truncation parameter $\alpha_0 = 0.1$, which are indeed normalizable with $\langle t \rangle = 0$. We chose a relatively small value of t_0 in order to bring out most clearly the essential features of the propagation dynamics [38]. For the analytic form of the Airy wave packet we refer to the appendix.

Figure 3(b) shows that the wavefront self-accelerates even for surface gravity water wave packets. The quantum potential depicted in figure 3(d) brings out the deeper reason: it exhibits a strong repulsive hill at the right corner, causing most trajectories to lean towards the opposite direction. Interestingly, the Bohm trajectories also reveal that the self-acceleration of the wavefront is a consequence of accelerating particles. However, there are also particles which decelerate, and move with almost constant negative velocity. As a result, the center of mass of the *entire* wave packet is maintained at $\langle t \rangle = 0$ thus, preserving the Ehrenfest condition.

4. Conclusions

In our article we have applied the Bohm interpretation of quantum waves relevant to the microscopic world to macroscopic surface gravity water waves and have gained deeper insight into their propagation dynamics. We have not only observed Bohm trajectories of two-and three-Gaussian slits and Airy wave packets but have also measured successfully the corresponding quantum potentials. Our experiments reveal that the shape of the quantum potential indeed dictates the propagation of the waves and provides a detailed visualization of their dynamics.

We emphasize that our experimental setup is neither limited to slits, nor to a free propagation. Indeed, it allows us to study the time evolution of an arbitrary wave packet, and even Bohmian mechanics in the presence of an external potential [25]. The methods we have demonstrated can be generalized to several other macroscopic types of waves including electromagnetic as well as acoustic waves.

Acknowledgments

It is with great pleasure that we dedicate this article to Prof Igor Jex on the occasion of his 60th birthday. One of us (W P S) is fortunate enough to have collaborated with Igor and his team for over thirty years on several topics and can testify to his deep insight into quantum phenomena, his incredible knowledge of the history of physics, and his wonderful Czech humor. Igor is not only a first-rate scientist and a dedicated teacher but above all, a great human being—a Mensch. Many thanks for our friendship! Happy Birthday Igor and many more healthy years together in science!

We thank Maxim A Efremov, Alona Maslennikov and Matthias Zimmermann for fruitful discussions. We also thank Tamir Ilan and Anatoliy Khait for technical support and assistance. This work was supported by the Israel Science Foundation, grants no. 1415/17, 969/22 and 508/19. D I B was supported by U S Army Research Office (ARO) grant W911NF-19-1-0377 and by a Humboldt Research Fellowship for Experienced Researchers from the Alexander von Humboldt Foundation. The views and conclusions contained in this document are those of the authors and should not be interpreted as representing the official policies, either expressed or implied, of ARO, or the U S Government. The U S Government is authorized to reproduce and distribute reprints for Government purposes notwithstanding any copyright notation herein.

Data availability statement

The data that support the findings of this study are available upon reasonable request from the authors.

Appendix. Wave function essentials

In this appendix we briefly elaborate on the data analysis and the form of the wave packets. First, we discuss the Hilbert transform and its relation to the imaginary part, as well as the phase and amplitude of the wave function. Second, we define the temporal envelopes of the initial wave packets used in our experiments.

A.1. Phase and amplitude measurement from Hilbert transform

In order to measure the imaginary part, phase and amplitude of the wave we use the Hilbert transform [32]. The amplitude and phase induced during the pulse propagation can be determined by creating a complex signal

$$z(t) \equiv u(t) + iv(t) \equiv u(t) + i \cdot \text{Hilbert}\{u(t)\} \tag{4}$$

from a real signal $u = u(t)$ with the help of the Hilbert transform

$$\text{Hilbert}\{u(t)\} \equiv \frac{1}{\pi}\int_{-\infty}^{\infty}\frac{u(s)}{t-s}ds. \tag{5}$$

Next, using the polar decomposition

$$z(t) \equiv A(t)e^{i\varphi(t)}, \tag{6}$$

we arrive at the instantaneous amplitude

$$A(t) \equiv \sqrt{u^2(t) + v^2(t)}, \tag{7}$$

and the instantaneous phase

$$\varphi(t) \equiv \arctan\left[\frac{v(t)}{u(t)}\right]. \tag{8}$$

We obtain $z = z(t)$ from the toolbox function 'hilbert' [41] of Matlab. This function computes the Hilbert transform for a real input sequence u, and returns a *complex* result of the same length, $z = \text{hilbert}(u)$, where the real part of z is the original real data and the imaginary part is the actual Hilbert transform defined by equation (5). In order to bring out most clearly the difference between the toolbox function 'hilbert' of Matlab and the Hilbert transform of equation (5) we use small and capital letters. We note that z is called the analytic signal, in reference to the continuous-time analytic signal.

A.2. Form of the initial wave packets

The temporal variation of the initial surface elevations $\eta^{(2)}$ and $\eta^{(3)}$ corresponding to the two-slit and three-slit experiments is based on Gaussian envelope slits of the form

$$\eta^{(2)}(t, 0) \equiv a_0\{\exp[-t^2/t_0^2] + \exp[-(t - t_s)^2/t_0^2]\}, \tag{9}$$

and

$$\eta^{(3)}(t, 0) \equiv a_0\{\exp[-t^2/t_0^2] + \exp[-(t - t_s)^2/t_0^2] + \exp[-(t + t_s)^2/t_0^2]\}, \tag{10}$$

respectively, where t_0 is the temporal width of the slits and t_s denotes the slit separation.

We also study the truncated Airy wave packets [35, 38] generated by the truncated Airy envelope

$$\eta^{(Ai)}(t, 0) \equiv a_0 \, \mathrm{Ai}\left(-\frac{t}{t_0}\right)\exp\left(-\alpha_0\frac{t}{t_0}\right), \tag{11}$$

where α_0 is the truncation parameter.

Finally, we analyze two slits with initial non-zero momenta [27], corresponding to wave packets generated by the two-slit function

$$\eta^{(2)}_{\pm p_0} \equiv \eta^{(2)}\exp(\pm i p_0 t), \tag{12}$$

with a negative or positive initial momentum p_0 and $\eta^{(2)}$ is given by equation (9).

ORCID iDs

Georgi Gary Rozenman https://orcid.org/0000-0002-0799-6520
Denys I Bondar https://orcid.org/0000-0002-3626-4804
Wolfgang P Schleich https://orcid.org/0000-0002-9693-8882
Lev Shemer https://orcid.org/0000-0003-0158-1823
Ady Arie https://orcid.org/0000-0001-6486-7285

References

[1] de Broglie L 1927 La mécanique ondulatorie et la structure atomique de lamati'ere et du rayonnement *Journal de Physique et du Radium* **8** 225
[2] Madelung E 1927 Quantentheorie in hydrodynamischer Form *Zeitschrift für Physik* **40** 322–6
[3] Bohm D 1952 A suggested interpretation of the quantum theory in terms of hidden variables I *Phys. Rev.* **85** 166
[4] Bohm D 1952 A suggested interpretation of the quantum theory in terms of hidden variables II *Phys. Rev.* **85** 180
[5] Bell J S 1992 Six possible worlds of quantum mechanics *Found. Phys.* **22** 1201
[6] Cramer J G 1986 The transactional interpretation of quantum mechanics *Rev. Mod. Phys.* **58** 647
[7] Holland P R 1993 *The Quantum Theory of Motion: An Account of the de Broglie-Bohm Causal Interpretation of Quantum Mechanics* (Cambridge: Cambridge University Press)
[8] Cushing J T, Fine A and Goldstein S 1996 *Bohmian Mechanics and Quantum Theory: An Appraisal, Boston Studies in the Philosophy of Science 184* (Netherlands: Springer)
[9] Scully M O 1998 Do Bohm trajectories always provide a trustworthy physical picture of particle motion? *Physica Scripta-Topical Volumes* **76** 41
[10] Nassar A B and Miret-Artés S 2017 *Bohmian Mechanics, Open Quantum Systems and Continuous Measurements* (Heidelberg: Springer)
[11] Dürr D and Teufel S 2009 *Bohmian Mechanics* (New York: Springer)
[12] Hojman S A, Asenjo F A and New A 2020 Approach to solve the one-dimensional Schrödinger equation using a wavefunction potential *Phys. Lett.* **A384** 126
[13] Asenjo F A, Hojman S A, Moya-Cessa H M and Soto-Eguibar F 2021 Propagation of light in linear and quadratic GRIN media: the Bohm potential *Opt. Com.* **490** 126947
[14] Zhdanov D V and Bondar D I 2022 Joint quantum-classical Hamilton variational principle in the phase space *J. Phys.* **55** 104001 A
[15] Albareda G, Suñé J and Oriols X 2009 Many-particle Hamiltonian for open systems with full Coulomb interaction: application to classical and quantum time-dependent simulations of nanoscale electron devices *Phys. Rev.* **79** 075315 B
[16] Oriols X 2007 Quantum-trajectory approach to time-dependent transport in mesoscopic systems with electron-electron interactions *Phys. Rev. Lett.* **98** 066803
[17] Benseny A, Albareda G, Sanz A S, Mompart J and Oriols X 2014 Applied Bohmian mechanics *Eur. Phys. J.* **68** 286 D
[18] Larder B *et al* 2019 Fast nonadiabatic dynamics of many-body quantum systems *Sci. Adv.* **5** eaaw1634
[19] Oriols X and Mompart J 2019 *Applied Bohmian Mechanics : From Nanoscale Systems to Cosmology* (Boca Raton: CRC Press)
[20] Schleich W P, Freyberger M and Zubairy M S 2013 Reconstruction of Bohm trajectories and wave functions from interferometric measurements *Phys. Rev.* **A87** 014102
[21] Dressel J, Malik M, Miatto F M, Jordan A N and Boyd R W 2014 Colloquium: understanding quantum weak values: basics and applications *Rev. Mod. Phys.* **86** 307

[22] Aharonov Y, Albert D Z and Vaidman L 1988 How the result of a measurement of a component of the spin of a spin-1/2 particle can turn out to be 100 *Phys. Rev. Lett.* **60** 1351

[23] Kocsis S *et al* 2011 Observing the average trajectories of single photons in a two-slit interferometer *Science* **332** 1170

[24] Mahler D H *et al* 2016 Experimental nonlocal and surreal Bohmian trajectories *Sci. Adv.* **2** e1501466

[25] Rozenman G G *et al* 2019 Amplitude and phase of wave packets in a linear potential *Phys. Rev. Lett.* **122** 124302

[26] Rozenman G G, Shemer L and Arie A 2020 Observation of accelerating solitary wavepackets *Phys. Rev.* E **101** 050201

[27] Rozenman G G *et al* 2021 Projectile motion of surface gravity water wave packets: an analogy to quantum mechanics *EPJ ST* **230** 931

[28] Rozenman G G, Schleich W P, Shemer L and Arie A 2022 Periodic wave trains in nonlinear media: Talbot revivals, Akhmediev breathers, and asymmetry breaking *Phys. Rev. Lett.* **128** 214101

[29] Mei C C 1983 *The Applied Dynamics of Ocean Surface Waves* (Hoboken: Wiley-Interscience)

[30] Shemer L and Dorfman B 2008 Experimental and numerical study of spatial and temporal evolution of nonlinear wave groups *Nonlinear Process. Geophys.* **15** 931

[31] Rozenman G G, Fu S, Arie A and Shemer L 2019 Quantum mechanical and optical analogies in surface gravity water waves *Fluids* **4** 96

[32] King F W 2009 *Hilbert Transforms* 1 (Cambridge, UK: Cambridge University Press)

[33] Griffiths D J 1998 *Introduction to Quantum Mechanics* (Hoboken: Wiley)

[34] Danon J and Nazarov Y 2013 *Advanced Quantum Mechanics* (Cambridge: Cambridge University Press)

[35] Berry M V and Balazs N 1979 Nonspreading wave packets *Am. J. Phys.* **47** 264

[36] Siviloglou G A and Christodoulides D N 2007 Accelerating finite energy Airy beams *Opt. Lett.* **32** 979

[37] Voloch-Bloch N, Lereah Y, Lilach Y, Gover A and Arie A 2013 Generation of electron Airy beams *Nature* **494** 331

[38] Fu S, Tsur Y, Zhou J, Shemer L and Arie A 2015 Propagation dynamics of Airy water-wave pulses *Phys. Rev. Lett.* **115** 034501

[39] Bar-Ziv U, Postan A and Segev M 2015 Observation of shape-preserving accelerating underwater acoustic beams *Phys. Rev.* B **92** 100301

[40] Weisman D, Carmesin C M, Rozenman G G, Efremov M A, Shemer L, Schleich W P and Arie A 2021 Diffractive guiding of waves by a periodic array of slits *Phys. Rev. Lett.* **127** 014303

[41] MATLAB Hilbert Transform Package https://mathworks.com/help/signal/ug/hilbert-transform.html